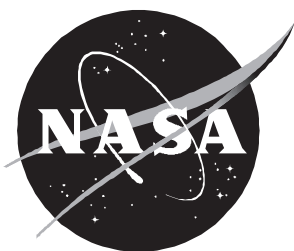# A Mathematical Model for Simulating Noise Suppression of Lined Ejectors

Willie R. Watson

A Mathematical Model for Simulating Noise Suppression of Lined Ejectors

Willie R. Watson
Langley Research Center • *Hampton, Virginia*

National Aeronautics and
Space Administration
Code JTT
Washington, D.C.
20546-0001

Abstract

A mathematical model containing the essential features embodied in the noise suppression of lined ejectors is presented. Although some simplification of the physics is necessary to render the model mathematically tractable, the current model is the most versatile and technologically advanced at the current time. A system of linearized equations and the boundary conditions governing the sound field are derived starting from the equations of fluid dynamics. A nonreflecting boundary condition is developed. In view of the complex nature of the equations, a parametric study requires the use of numerical techniques and modern computers. A finite element algorithm that solves the differential equations coupled with the boundary condition is then introduced. The numerical method results in a matrix equation with several hundred thousand degrees of freedom that is solved efficiently on a supercomputer. The model is validated by comparing results either with exact solutions or with approximate solutions from other works. In each case, excellent correlations are obtained. The usefulness of the model as an optimization tool and the importance of variable impedance liners as a mechanism for achieving broadband suppression within a lined ejector are demonstrated.

Introduction

The number of airplane passengers traveling in the long-range international market is expected to quadruple within 25 years. International travel experts agree that an environmentally acceptable and economically viable supersonic transport could obtain nearly 30 percent of this lucrative market. This forecast has given development of a high-speed civil transport (HSCT) a new impetus within the United States, Europe, and the Orient. Such an airplane could be expected to fly as soon as the early part of the next century and to cruise at speeds between Mach 2 and Mach 3. The first country to put such a technology in place would be in a leadership position in long-range civil aviation for many years to come. NASA and several private companies have taken up the challenge of putting such a technology in place for the United States. The current focus of NASA is on ozone depletion and noise; the latter is the subject of this paper.

To become environmentally acceptable, the HSCT must achieve noise levels comparable to those of other large commercial airplanes expected to fly during that period. Several studies (refs. 1–5) show that a reduction of 20 decibels in the radiated noise levels on takeoff will be required before the HSCT will meet stage-III noise standards. The mixer-ejector exhaust component is expected to provide one means of reducing the jet noise by mixing the high-velocity gases of the exhaust jet with much cooler ambient air; the result is a stream of air with a lower noise and energy level. The mixer-ejector is expected to provide only about 12 of the 20-dB reduction requirement. (See refs. 6–9.) Thus, a second component, which is expected to be a lined ejector, will be required to bring the radiated noise to environmentally acceptable levels.

Experimental tests, which would be required to develop an acceptable lined ejector technology, are expensive in terms of both research dollars and time. Accurate mathematical models for predicting and minimizing the noise field within a lined ejector can be important in this development. These models could be used as inexpensive, nonlabor-intensive technology tools to optimize the lining for maximum noise suppression, to explore more innovative lining concepts, and to minimize expensive experimental tests. Mathematical models currently exist for predicting liner noise suppression properties in flow; these models are restricted mostly to

irrotational subsonic flow and to sources that are tonal in nature such as fan noise. Several articles representing only a portion of what is available have been cited in references 10–15. Present mathematical models are not applicable for the analysis of the lined ejector noise suppression because they do not properly account for the characteristics of the jet exhaust that will generate this complex noise field.

The exhaust jet of the HSCT is expected to flow within a rectangular domain and will consist of an extremely hot supersonic core superimposed above and below with a cooler subsonic flow. The high-frequency broadband noise generated by the intense mixing of this composite flow field within the ejector escapes to the far field. This portion of the noise spectrum is targeted for reduction by the lined ejector. Aspects of liner noise reduction that are new to this environment include a rotational composite flow field and an extremely hot flowing gas. In addition, the jet noise source is distributed, broadbanded, and more directed than noise sources considered to date. Variable impedance liners, as considered in this work, are expected to be an essential component for attenuation of broadband jet noise. (See refs. 16 and 17.) An intense literature search produced no mathematical models for predicting the attenuation in this expected environment. Note that in the 1970's, Abrahamson (refs. 18 and 19) developed the most promising mathematical model for analyzing rotational flows in acoustically treated ducts with variable impedance liners. However, this model is restricted to subsonic flow and circular axisymmetric geometries, tailored to fan duct noise sources, and developed for a computer system that is more than 25 years old. Furthermore, recent analyses (ref. 20) show that an additional boundary condition is required for accurate solutions to vortical flow problems.

This paper describes a new mathematical model that simulates the essential characteristics of noise suppression with lined ejectors. A system of equations governing the sound field in a viscous, composite, vortical flow field is derived starting from the equations of fluid dynamics. Boundary conditions (including a new nonreflecting condition) consistent with this system are then introduced. A numerical method solves the differential equations with boundary conditions on a supercomputer. Several example problems are modeled and the results compared with their exact analytical solutions; comparisons with other approximate solution methods are made when exact solutions are not possible. Supersonic flow analysis is validated by comparing the model results with the results of a recently developed modal theory for plug flow. (See ref. 21.) Finally, the usefulness of the model as an optimization tool is tested. The model is also used to show the importance of variable impedance liners as a mechanism for achieving broadband noise suppression within an ejector.

Problem Formulation

A typical jet exhaust enshrouded by a lined ejector is illustrated in figure 1. The fluid within the mixing duct is considered to be viscous, composite, laminar, and compressible. The flow field within the ejector is considered a composite of subsonic and supersonic flow. To reduce computational requirements for the solution, only two-dimensional flow is considered; no variations in the flow occur in the direction normal to the X-Y plane. The inflow and outflow boundaries are at $x = 0$ and $x = L$, respectively. Sound sources occurring within the region $0 \leq x \leq L$ will be modeled accordingly. The lower and upper boundaries at $y = 0$ and $y = H$, respectively, contain the wall lining. Noise suppression properties of the lining are specified by the normal acoustic impedances of the upper and lower walls, z_H and z_0, respectively. These impedances are functions of the frequency content of the acoustic waves, position along the wall, and steady-state flow Mach number. In this paper, a numerical method is described for predicting the sound attenuation within the lined region $0 \leq x \leq L$ and for optimizing the wall lining.

Governing Equations

The two-dimensional Navier-Stokes equations which govern the fluid flow within the domain described in figure 1 are

$$\frac{\partial \{U\}}{\partial t} + \frac{\partial \{H\}}{\partial x} + \frac{\partial \{G\}}{\partial y} = \{0\} \tag{1}$$

The vectors in equation (1) are defined elsewhere (e.g., ref. 22) and are not repeated here. The unknown variables in $\{U\}$ are the fluid density ρ, axial component of velocity u, transverse component of velocity v, and total energy E.

To derive the equations governing acoustic disturbances in the total flow field, the unknown fluid variables are resolved into the following steady flow field and steady-state acoustic field components:

$$\{\Phi\} = \{\Phi_0\} + \{\widetilde{\Phi}\}e^{i\omega t} \qquad \omega = 2\pi f \tag{2a}$$

$$\{\Phi\} = \begin{Bmatrix} \rho \\ u \\ v \\ p \end{Bmatrix} \qquad \{\Phi_0\} = \begin{Bmatrix} \rho_0 \\ u_0 \\ v_0 \\ p_0 \end{Bmatrix} \qquad \{\widetilde{\Phi}\} = \begin{Bmatrix} \tilde{\rho} \\ \tilde{u} \\ \tilde{v} \\ \tilde{p} \end{Bmatrix} \tag{2b}$$

where vectors $\{\Phi\}$, $\{\Phi_0\}$, and $\{\widetilde{\Phi}\}$ contain the total flow field, steady flow field, and steady-state acoustic field in the flow, respectively. Here, f is the frequency in hertz and $i = \sqrt{-1}$. The following observations are made concerning equations (2): the steady flow field is a function of both spatial coordinates and the normal assumptions for parallel and/or irrotational duct flow are not made; the axially propagating wave assumption is not assumed, which means that vortical acoustic disturbances are possible; and an ideal gas is assumed which eliminates temperature as a variable.

After substituting equations (2) in equation (1), the following linearized system governing the acoustic disturbances in the flow field is obtained:

$$[A_0]\frac{\partial \{\widetilde{\Phi}\}}{\partial x} + [B_0]\frac{\partial \{\widetilde{\Phi}\}}{\partial y} + [G_0]\{\widetilde{\Phi}\} = \{0\} \tag{3a}$$

$$[A_0] = \begin{bmatrix} u_0 & \rho_0 & 0 & 0 \\ 0 & u_0 & 0 & \frac{1}{\rho_0} \\ 0 & 0 & u_0 & 0 \\ 0 & \rho_0 c_0^2 & 0 & u_0 \end{bmatrix} \qquad [B_0] = \begin{bmatrix} v_0 & 0 & \rho_0 & 0 \\ 0 & v_0 & 0 & 0 \\ 0 & 0 & v_0 & \frac{1}{\rho_0} \\ 0 & 0 & \rho_0 c_0^2 & v_0 \end{bmatrix} \tag{3b}$$

$$[G_0] = \begin{bmatrix} \left(i\omega + \frac{\partial u_0}{\partial x} + \frac{\partial v_0}{\partial y}\right) & \frac{\partial \rho_0}{\partial x} & \frac{\partial \rho_0}{\partial y} & 0 \\ \left(\frac{u_0}{\rho_0}\frac{\partial u_0}{\partial x} + \frac{v_0}{\rho_0}\frac{\partial u_0}{\partial y}\right) & \left(i\omega + \frac{\partial u_0}{\partial x}\right) & \frac{\partial u_0}{\partial y} & 0 \\ \left(\frac{u_0}{\rho_0}\frac{\partial v_0}{\partial x} + \frac{v_0}{\rho_0}\frac{\partial v_0}{\partial y}\right) & \frac{\partial v_0}{\partial x} & \left(i\omega + \frac{\partial v_0}{\partial y}\right) & 0 \\ 0 & \frac{\partial p_0}{\partial x} & \frac{\partial p_0}{\partial y} & \left(i\omega + \gamma\frac{\partial u_0}{\partial x} + \gamma\frac{\partial v_0}{\partial y}\right) \end{bmatrix} \tag{3c}$$

The ambient speed of sound c_0 is defined by

$$c_0^2 = \frac{\gamma p_0}{\rho_0} \tag{4}$$

Equations (3) may be interpreted as the linearized steady-state counterpart of that derived in reference 20.

The effects of nonlinearity, viscosity, and heat conduction are important in establishing the steady flow field and sources of sound, but they are not of primary importance in determining the steady-state acoustic disturbances discussed in this paper. Although some solutions of equation (1) for a general initial condition contain both the steady-state and the transient wave fields, viscous forces present in equation (1) will rapidly dissipate the transient wave field and leave only the steady-state acoustic field of equations (3) as the dominant noise field. Note that determination of the steady flow field $\{\Phi_0\}$ is necessary for solution of the acoustic problem, but the assumptions and techniques used to obtain this solution are not part of this work. Instead, the steady flow field is assumed to be available in a form suitable for inclusion into this equation. Finally, before equation (3a) can be solved, a set of boundary conditions consistent with this system must be specified.

The computational domain consists of two physical boundaries (the acoustically lined walls) and two artificial or free boundaries (the inflow and outflow boundary). The solution of the acoustic problem requires three boundary conditions along the subsonic portion of the inflow boundary and four along the supersonic portion. (See ref. 20.) Note that in references 18 and 19, only two boundary conditions were imposed at the subsonic inflow boundary. In general, two boundary conditions are insufficient for acoustic calculations in vortical flows. Along the outflow boundary, no boundary condition is needed for the supersonic portion; however, a single boundary condition is required along the subsonic portion.

As a result, along the inflow boundary acoustic pressure and tangential component of acoustic velocity are specified and the disturbance is assumed homentropic as follows:

$$\tilde{p}(0, y) = p_s(y) \tag{5a}$$

$$\tilde{v}(0, y) = v_s(y) \tag{5b}$$

$$\tilde{p}(0, y) = c_0^2(0, y)\tilde{\rho}(0, y) \tag{5c}$$

In equations (5a) and (5b), $p_s(y)$ and $v_s(y)$ are the source acoustic pressure and tangential component of acoustic velocity, respectively, at the inflow boundary; equation (5c) is the homentropic inflow condition. In addition to equations (5), two conditions are required: one along any supersonic portion of the inflow boundary and one along the subsonic part of the outflow boundary. These additional conditions are presented after the discussion of the numerical method.

The acoustic boundary condition at the treated walls must be determined by the nature of the interaction of the acoustic waves and the mechanical structure forming the wall. Low-speed subsonic flow can possibly result in the ratio of acoustic pressure to the normal component of acoustic velocity at the surface assuming a specified value, which is referred to as the normal acoustic impedance. Whether this can be achieved for a composite flow containing an extremely hot flowing gas is currently a research issue. The current model assumes that a locally reacting surface impedance can be defined for the lining material even in this new environment. For no slip at the liner and flow interface, the condition can be stated as

$$\frac{\tilde{p}(x, 0)}{\tilde{v}(x, 0)} = -z_0(x) \tag{6a}$$

$$\frac{\tilde{p}(x, H)}{\tilde{v}(x, H)} = z_H(x) \tag{6b}$$

4

Occasionally, a uniform or plug flow model will be convenient to permit fluid slip at the wall. The proper form of the wall boundary condition (ref. 23) for this situation is

$$\tilde{v}(x,0) = -\frac{\tilde{p}(x,0)}{z_0(x)} - \frac{u_0(x,0)}{i\omega}\frac{\partial}{\partial x}\left[\frac{\tilde{p}(x,0)}{z_0(x)}\right] \tag{7a}$$

$$\tilde{v}(x,H) = \frac{\tilde{p}(x,H)}{z_H(x)} + \frac{u_0(x,H)}{i\omega}\frac{\partial}{\partial x}\left[\frac{\tilde{p}(x,H)}{z_H(x)}\right] \tag{7b}$$

where the component of the steady velocity v_0 in the Y direction is assumed zero at the wall. As expected, equations (7) reduce to equations (6) when there is no slip at the wall.

Equations (3) describe linear acoustic disturbances in viscous, rotational, and compressible fluid flow. Note that in the absence of any disturbance, equation (3a) is satisfied identically. No exact analytical solutions of these equations exist for an arbitrary steady flow. The method chosen to solve the acoustic equations (3) coupled with boundary conditions defined by equations (4)–(7) is a Galerkin finite element method, which is discussed in the following section.

Galerkin Finite Element Analysis

Details on the finite element theory may be found in several texts. (See, for example, refs. 24 and 25.) The finite element method, when applied to the current acoustic problem, represents the continuous sound field as an assemblage of rectangular elements interconnected at nodes as illustrated in figure 2(a): N nodes in the axial direction and M nodes in the transverse direction. Note that the acoustic field is zoned at imaginary lines although no physical separation is envisioned. A typical rectangular element e is shown in figure 2(b). Each element consists of four nodes labeled 1, 2, 3, and 4, respectively, and is considered to have width a and height b. Values of a and b for each element should be chosen so that the acoustic disturbances and steady flow field within each element are simulated as closely as possible. The objective is to obtain the unknown acoustic variables at the nodes of each of the $(M-1)$, $(N-1)$ elements.

Galerkin's finite element method is used to minimize the error vector and reduces the problem to a finite set of algebraic equations which are solved using matrix methods. The error vector is defined as

$$\{E_r(x,y)\} = [A_0]\frac{\partial\{\widetilde{\Phi}\}}{\partial x} + [B_0]\frac{\partial\{\widetilde{\Phi}\}}{\partial y} + [G_0]\{\widetilde{\Phi}\} \tag{8}$$

Within each element, the acoustic pressure, two components of acoustic velocity, and the density will be represented as the following linear functions:

$$\tilde{p}(x,y) = \sum_{J=1}^{4} N_J(x,y)\tilde{p}_J \qquad \tilde{u}(x,y) = \sum_{J=1}^{4} N_J(x,y)\tilde{u}_J \tag{9a}$$

$$\tilde{v}(x,y) = \sum_{J=1}^{4} N_J(x,y)\tilde{v}_J \qquad \tilde{\rho}(x,y) = \sum_{J=1}^{4} N_J(x,y)\tilde{\rho}_J \tag{9b}$$

$$N_1(x,y) = \left(1 - \frac{x}{a}\right)\left(1 - \frac{y}{b}\right) \qquad N_2(x,y) = \frac{x}{a}\left(1 - \frac{y}{b}\right) \tag{9c}$$

$$N_3(x,y) = \frac{x}{a}\frac{y}{b} \qquad N_4(x,y) = \left(1 - \frac{x}{a}\right)\frac{y}{b} \tag{9d}$$

5

in which $\tilde{p}_J$, $\tilde{u}_J$, $\tilde{v}_J$, and $\tilde{\rho}_J$ are the values of acoustic pressure, axial component of acoustic velocity, transverse component of acoustic velocity, and acoustic density at node J, respectively. The steady flow field is represented in a similar manner as

$$p_0(x,y) = \sum_{J=1}^{4} N_J(x,y)P_J \qquad u_0(x,y) = \sum_{J=1}^{4} N_J(x,y)U_J \qquad (9e)$$

$$v_0(x,y) = \sum_{J=1}^{4} N_J(x,y)V_J \qquad \rho_0(x,y) = \sum_{J=1}^{4} N_J(x,y)R_J \qquad (9f)$$

The correct solution of equations (3) for the acoustic system is obtained when the error vector $\{E_r(x,y)\}$ is identically zero at each point of the domain. An approximate solution is achieved by requiring that the error vector be orthogonal to each basis function $N_J(x,y)$ that is assumed to represent a complete set of functions. The contribution of a typical element to the minimization of the error function is

$$\int_0^a \int_0^b \{E_r(x,y)\} N_J(x,y)\,dy\,dx = [A^e]\{\Phi^e\}$$

in which $[A^e]$ is a 16 $\times$ 16 complex matrix (i.e., the stiffness matrix) and $\{\Phi^e\}$ is a 16 $\times$ 1 column vector containing the unknown acoustic variables at the four nodes of the element. The coefficients in the local stiffness matrix $[A^e]$ were computed in closed form and are not included in this report.

Assembly of the global stiffness matrix for the computational domain is a basic procedure in the finite element method. Appropriate shifting of rows and columns is all that is required to add the local element $[A^e]$ directly into the global matrix $[A]$. Assembling the elements for the entire domain results in a matrix equation of the form

$$[A]\{\Phi\} = \{F\} \qquad (10)$$

in which $[A]$ is a $4MN \times 4MN$ complex matrix, and $\{\Phi\}$ is a $4MN \times 1$ column vector containing the nodal values of the unknown acoustic variables. In equation (10), the $4MN \times 1$ column vector $\{F\}$ is identically zero and the global stiffness matrix $[A]$ is singular. Therefore, boundary conditions must be applied to this system of equations before a solution can be obtained.

As mentioned in the previous section, an additional condition must be specified before the solution can be calculated. Determining the inflow or outflow boundary condition is difficult. The difficulty arises because the sound field within the ejector propagates through the multidimensional steady flow field and radiates outward to the surrounding environment. The additional boundary condition must model this characteristic. Several methods have been proposed for determining this boundary condition in subsonic flows. Abrahamson (refs. 18 and 19) expressed this boundary condition as a local linear relationship between the acoustic pressure and the normal component of acoustic velocity. The method of determining the constant in this linear relationship was not specified. Horowitz, Sigman, and Zinn (ref. 26) expressed this boundary condition in terms of an exit impedance. Because the exit impedance was not known *a priori*, the solution within the finite computational domain was combined with an integral formulation for the far field. The exit impedance was then compared with that obtained from the integral formulation at the boundary and was iteratively corrected until the results converged. A similar method was applied by Baumeister. (See ref. 27.)

In this report, the additional condition is expressed as a linear relationship between the acoustic pressure at a boundary node and the normal component of acoustic velocity along the boundary nodes:

$$\{PB\} = [Z]\{UB\} \tag{11a}$$

$$[Z] = \begin{bmatrix} Z_{11} & Z_{12} & \ldots & Z_{1M} \\ Z_{21} & Z_{22} & \ldots & Z_{2M} \\ \vdots & \vdots & \ddots & \vdots \\ Z_{M1} & Z_{M2} & \ldots & Z_{MM} \end{bmatrix} \tag{11b}$$

Here $\{PB\}$ and $\{UB\}$ are $1 \times M$ column vectors containing the acoustic pressure and the normal component of acoustic velocity, respectively, along the boundary nodes. Determining the complex coefficients in the $M \times M$ matrix $[Z]$ is difficult for the general case. The elements in this matrix should result in the acoustic field having the correct radiation condition. The coefficients in $[Z]$ that ensure no reflections are derived in the appendix. This derivation assumes that the duct terminates in an environment that is homogeneous in the axial direction. Alternatively, $[Z]$ could be obtained by an extension of the iterative method proposed in reference 26.

Numerical Implementation of Boundary Conditions

Along the boundaries of the computational domain, three types of boundary conditions may exist: the noise source pressure or tangential velocity, the homentropic acoustic wave condition of equation (5c), or the additional condition of equations (11). All three boundary conditions can be inserted into the assembled global matrix equation (10) by imposing relations on the nodal values of acoustic variables along the boundary. Details for imposing the boundary conditions are described in references 18, 24, and 25 and are not repeated here. The noise source boundary condition consists simply of specifying all nodal values of acoustic pressure or velocity. The homentropic acoustic wave condition involves specifying a linear relationship between acoustic pressure and acoustic density at the inflow boundary nodes. The additional condition in equations (11) involves specifying a linear relationship between acoustic pressure at a node and the normal component of acoustic velocity at the boundary nodes.

Solution to the Matrix Equation

The global matrix $[A]$, generated by Galerkin's method after the application of boundary conditions, is an unsymmetric, positive indefinite, complex matrix. Fortunately, because of the discretization method used, the matrix will be square and block tridiagonal of order $4MN$; the structure of matrix $[A]$ is shown in figure 3(a). This global matrix contains a number of major blocks a_J, b_J, and c_J that are square and block tridiagonal and have the structure shown in figure 3(b). Each minor block A_J, B_J, and D_J is a square matrix the order of which is four. Of practical significance, the structure minimizes computer storage requirements and maximizes computational efficiency. All computation, storage, and boundary condition manipulations are performed on the block triangular portion only of the matrix $[A]$. (See fig. 3(a).) Special matrix techniques exist for a solution of this structure. Gaussian elimination with partial pivoting and equivalent row infinity norm scaling is used to reduce the rectangular system to an upper triangular form. Back-substitution is then employed to obtain the solution for the acoustic variables. All computations were performed on the supercomputer.

Evaluation of Liner Performance

A primary objective of the numerical method is to evaluate the performance of the wall lining. The following uniform flow expression (ref. 28) is used for the acoustic intensity at a

point (x, y) in a uniform steady flow:

$$I(x,y) = \frac{1}{4}(\tilde{p}\tilde{u}^* + \tilde{p}^*\tilde{u}) + \frac{M_0}{4}\rho_0 c_0 \left(\tilde{u}\tilde{u}^* + \tilde{v}\tilde{v}^* + \frac{\tilde{p}\tilde{p}^*}{\rho_0 c_0}\right) \tag{12}$$

The steady flow Mach number M_0 is defined as u_0/c_0 and the superscript asterisk denotes the complex conjugate. The attenuation of the lining in decibels is then obtained from the equations

$$\Delta\mathrm{dB} = 10\log_{10}\frac{W(0)}{W(L)} \tag{13a}$$

$$W(x) = \int_0^H I(x,y)\,dy \tag{13b}$$

To obtain the axial acoustic energy flux $W(x)$, the integration in equation (13b) was performed in closed form. Equations (13) are used to evaluate the effect of the wall lining in this report; results in the next section are purposely restricted to uniform flow.

Results and Discussion

To validate the numerical model, finite element method results are compared with exact analytical results for a rigid wall duct and with an approximate modal theory recently developed for uniform supersonic flow between soft walls. (See ref. 21.) These solutions are compared for a range of frequencies and Mach numbers. Such comparisons provide confidence in the boundary condition formulation, convergence characteristics, computational cost, and overall accuracy of the numerical model. The model was also used to perform optimization studies and to demonstrate that the variable impedance liner is a candidate for enhancing the broadband performance of lined ejectors.

Results for a Rigid Wall Duct

For a rigid wall duct $(z_0(x) = z_H(x) \to \infty)$ with uniform flow in the positive X direction, the acoustic pressure field consisting only of a simple progressive single mode is

$$\tilde{p}(x,y) = A_m \cos\left(\frac{m\pi y}{H}\right) e^{iK_m x} \tag{14}$$

where K_m satisfies the condition

$$K_m = \frac{-kM + \sqrt{k^2 M^2 + (1-M^2)\left[k^2 - \left(\frac{m\pi}{H}\right)^2\right]}}{M^2 - 1} \qquad (m = 0, 1, 2, ..., \infty)$$

and

$$M = \frac{u_0}{c_0} \qquad k = \frac{\omega}{c_0}$$

Equation (14) may be regarded as a special solution of equations (3) with

$$p_s(y) = A_m \cos\left(\frac{m\pi y}{H}\right) \qquad \tilde{p} = c_0^2 \tilde{\rho} \qquad v_s(y) = \frac{ip_s'(y)}{\rho_0(\omega + K_m u_0)}$$

The matrix $[Z]$, which ensures the existence of a simple progressive traveling wave, is

$$[Z] = -\frac{\rho_0(\omega + K_m u_0)}{K_m}[I]$$

8

where $[I]$ is the identity matrix and only a single mode m is assumed to propagate. The above is a standard result that is based on a constant steady flow field and is computed by separation of variables. The solution is useful for comparison with numerical calculations. Numerical results for a rigid wall duct were computed with ambient values of p_0, ρ_0, and T_0, with $L = H = 0.5$ m and $A_m = 1$; and with an evenly spaced 51×51 mesh. Results were computed for a subsonic and supersonic Mach number ($M_0 = 0.5$ and $M_0 = 1.5$), three frequencies ($f = 500$ Hz, $f = 5000$ Hz, and $f = 10\,000$ Hz), and a planar ($m = 0$) and nonplanar ($m = 1$) source. Although several transverse and axial locations were checked at random in the duct, results are shown only for the transverse location $y = 0.75H$ to limit the number of graphs.

Graphs of the real and imaginary solutions for the planar ($m = 0$) acoustic pressure computed from this analysis are compared with the exact steady state solution for the subsonic and supersonic Mach number in figures 4 and 5, respectively. Computations are for a frequency of 500 Hz and excellent correlation was obtained between the exact and numerical solution. No reflections as a result of the chosen boundary condition are evident in the figures. However, note that the wavelength of the acoustic wave in the supersonic flow has been stretched compared with that of the subsonic flow. Thus, the number of computational points required for accurate resolution may be considerably less for sound waves in a supersonic flow.

Results are shown in figures 6 and 7 when the frequency of the planar wave is increased an order of magnitude ($f = 5000$ Hz). Again, excellent correlation was obtained for the subsonic and supersonic Mach number. Note that for the subsonic Mach number, approximately 10 axial points per wavelength (i.e., $N = 51$) are used in the finite element computer code. The 10 axial points per wavelength are considered the least number of axial nodes for which an accurate numerical solution can be expected in the subsonic flow. Figure 8 shows the results for the supersonic Mach number at the highest frequency ($f = 10\,000$ Hz). Good correlation is again obtained. Numerical results were also obtained for a nonplanar ($m = 1$) wave source at all three frequencies. Figure 9 shows a sample calculation for the nonplanar wave at the highest frequency ($f = 10\,000$ Hz) and the supersonic Mach number. Good correlation between the finite element and exact solutions is obtained; better correlation than that of figure 9 was obtained at the two lower frequencies, although results are not shown for the sake of brevity.

Results With Wall Lining

Lining materials used in the ejector of the HSCT should have the following characteristics: have minimum thickness and weight, resist high pressures, withstand extreme temperatures, and absorb broadband sound. Results in the previous section confirmed that the mathematical model can be used to calculate in detail the sound field for planar and nonplanar acoustic waves. In this section, the application of the model for prediction of the sound attenuation of a wall lining is discussed. Although no exact solutions are possible for vortical flow, an approximate modal solution is possible in uniform flow. This modal solution has been explored in detail by several other researchers for subsonic flows. Recently, the modal solution (ref. 21) was expanded to include uniform supersonic flow. This modal solution is used as a basis to test predictions of the model discussed in this report. Because data will soon be available from ejector tests to be performed in the Langley Jet Noise Facility, the geometry of that facility (i.e., $L = 0.3302$ m and $H = 0.127$ m) was used to develop the results that follow. Further, a 51×51 evenly spaced grid was used in all calculations.

A comparison of the finite element model attenuation predictions with the modal theory was made for a planewave source (i.e., $p_s(y) = 1$) at 1500 Hz with $z_H = z_0 = 2 - 0.58i$. The modal

theory represented the source pressure with a four-mode expansion. Comparisons were made by using the following $[Z]$ matrix:

$$[Z] = \begin{bmatrix} z_1 & 0 & \ldots & 0 \\ 0 & z_2 & \ldots & 0 \\ \vdots & \vdots & \ddots & \vdots \\ 0 & 0 & \ldots & z_M \end{bmatrix}$$

in which

$$z_i = \frac{\tilde{p}(x, y_i)}{\tilde{u}(x, y_i)}$$

Values of $\tilde{p}(x, y_i)$ and $\tilde{u}(x, y_i)$ were computed from the four-mode expansion. The matrix $[Z]$ above has the advantage that only four modes in the lined section have to be computed. The disadvantage of this choice of $[Z]$ is that it requires prior knowledge of the solution. Note that although the full matrix $[Z]$ as derived in the appendix is preferred, the 51 soft wall modes required for the computation were not readily available from the modal theory.

Results are plotted as a function of Mach number in figure 10. As shown, the attenuation is reduced with increasing Mach number even in the supersonic flow. Again, note that liner attenuation in supersonic flow as considered here represents a new development. Further, the finite element and modal theory show no discrepancy in the subsonic flow. Both predictions correlate closely in the supersonic flow region, although the small oscillation that occurs in the finite element results is not characteristic of the modal theory. Similar characteristics were observed for most of the other frequency values.

An Optimization Study on Broadband Suppression

The HSCT requires that special attention be given to optimization of liner properties. Unlike fan noise sources that are tonal in nature, jet sources are distributed and broadband. The impedance of a lined ejector must be determined so that maximum broadband suppression is achieved. The present model is applicable to such an extensive and thorough parametric study. To demonstrate the mathematical model for this purpose, an analysis to optimize a uniform lining impedance was completed. An optimal uniform liner has been obtained by mapping contours in the complex impedance plane. A segmented lining was then developed which had greater broadband suppression than that of an optimal uniform lining.

Figure 11(a) shows a variable impedance liner designed to enhance the broadband performance of the ejector. For simplicity, a two-segmented liner with each segment $0.5L$ units long has been chosen. Channel dimensions (L and H) were equivalent to those of the ejector located in the Langley Jet Noise Laboratory. The impedances of the first and second segment of the segmented liner were not optimized but were taken from the finite element model results of the individual uniform liner optimization studies in a supersonic flow.

Figure 11(b) shows the result of the design at $M_0 = 1.5$ and frequencies of 0–10 000 Hz. A $\rho_0 c_0$ entrance impedance and a planar source pressure have been assumed. The curve data for the two uniform liners were computed by giving each segment in figure 11(a) the same wall impedance. The uniform liner was then optimized for maximum suppression at a fixed frequency defined as the tuning frequency. Both optimized uniform liners were observed to perform well at their tuning frequency but their performances fall off rapidly on either side of their tuning frequency. This characteristic is clearly undesirable for the broadband jet noise source which would occur in an ejector. Attenuation predictions for the segmented liner with the first segment tuned at 2500 Hz and the second segment tuned at 5000 Hz are also shown in the figure. The segmented liner suppresses more high-frequency sound than the uniform liner tuned at 2500 Hz and more

low-frequency sound than the uniform liner tuned at 5000 Hz. Therefore, the segmented liner is more desirable for a broadband jet noise source. If the impedance of the first and second segment were actually optimized, the attenuation spectrum for the segmented liner could be much broader.

Conclusions

The objective of this report was to introduce the equations and develop the numerical method for predicting and optimizing the noise suppression of lined ejectors. A complete validation of the full capability of the model in a single report is not possible; the results were purposely restricted to irrotational flows because exact and approximate solutions are available in the literature for comparison and an expression for the liner performance is known. Validation of the model in a vortical flow field has not yet been accomplished and is beyond the scope of this report. Results from the model to date are satisfactory and show expected convergence characteristics over a wide range of frequencies, Mach numbers, and source conditions.

The following specific conclusions are based upon these results:

1. A mathematical model believed to contain the essential features required for predicting sound suppression by lined ejectors is developed.

2. The model is compatible with a composite flow field (vortical and nonvortical), variable impedance liners, arbitrary noise sources, and the current generation of supercomputers.

3. Although a simplification of the physics has been necessary to make the problem mathematically tractable, the current model is the most versatile and technologically advanced at the present time.

4. Excellent correlation with the exact solution for planar and nonplanar sources in subsonic and supersonic flow in a rigid wall duct is obtained using approximately 10 points per wavelength.

5. Results with wall lining show excellent correlation with a recently developed modal theory (ref. 21) for uniform supersonic flow.

6. The use of the model as an optimization tool is successfully demonstrated.

7. Optimization studies with the model confirm the advantage of variable impedance liners as a possible mechanism for achieving broadband noise suppression in lined ejectors.

References

1. Tirumalesa, Duvvuri: Theoretical Analysis of the Noise Characteristics of an Ejector Jet. *J. Sound & Vib.*, vol. 30, no. 4, 1973, pp. 465–481.

2. Middleton, D.: Theoretical and Experimental Investigations Into the Acoustic Output From Ejector Flows. *J. Sound & Vib.*, vol. 11, no. 4, 1970, pp. 447–473.

3. Huff, Ronald G.; and Groesbeck, Donald E.: *Geometric Factors Affecting Noise Suppression and Thrust Loss of Divergent-Lobe Supersonic Jet Noise Suppressor.* NASA TM X-2820, 1973.

4. Atvars, J.; Wright, C. P.; and Simcox, C. D.: Supersonic Jet Noise Suppression With Multitube Nozzle/Ejectors. AIAA-75-501, Mar. 1975.

5. Ahuja, K. K.; Manes, J. P.; Massey, K. C.; and Calloway, A. B.: An Evaluation of Various Concepts of Reducing Supersonic Jet Noise. AIAA-90-3982, Oct. 1990.

6. Lord, W. K.; Jones, C. W.; and Stern, A. M.: Mixer Ejector Nozzle for Jet Noise Suppression. AIAA-90-1909, July 1990.

7. Presz, Walter M., Jr.: Mixer/Ejector Noise Suppressors. AIAA-91-2243, June 1991.

8. Seiner, John M.; and Krejsa, Eugene A.: Supersonic Jet Noise and the High Speed Civil Transport. AIAA-89-2358, July 1989.

9. Tanner, D. D.; and Wynosky, T. A.: *Fabrication and Instrumentation of Scale Model Hyper-Mix Ejector Nozzle STOVL Exhaust System.* PW FR-21494, Oct. 1990.

10. Nayfeh, Ali H.; Kaiser, John E.; and Telionis, Demetri P.: Acoustics of Aircraft Engine-Duct Systems. *AIAA J.*, vol. 13, no. 2, Feb. 1975, pp. 130–153.

11. Kraft, Robert Eugene: Theory and Measurement of Acoustic Wave Propagation in Multi-Segmented Rectangular Flow Ducts. Ph.D. Diss., Univ. of Cincinnati, 1976.

12. Baumeister, K. J.: Time Dependent Difference Theory for Sound Propagation in Axisymmetric Ducts With Plug Flow. AIAA-80-1017, June 1980.

13. Baumeister, K. J.: Numerical Techniques in Linear Duct Acoustics—A Status Report. Trans. ASME, *J. Eng. Ind.*, vol. 103, no. 3, Aug. 1981, pp. 270–281.

14. Zorumski, William E.: *Acoustic Theory of Axisymmetric Multisectioned Ducts.* NASA TR R-419, 1974.

15. Rice, Edward J.; Heidmann, Marcus F.; and Sofrin, Thomas G.: Modal Propagation Angles in a Cylindrical Duct With Flow and Their Relation to Sound Radiation. AIAA-79-0183, Jan. 1979.

16. Wirt, L. S.: The Design of Sound Absorptive Materials To Meet Special Requirements. *J. Acoust. Soc. America*, vol. 51, no. 5, pt. 1, May 1972.

17. Jones, Michael G.; and Parrott, Tony L.: Noise Control in Aeroacoustics—Proceedings of Noise-Con 93. Harvey H. Hubbard, ed., Inst. Noise Control Eng., 1993, pp. 279–284.

18. Abrahamson, A. L.: *A Finite Element Algorithm for Sound Propagation in Axisymmetric Ducts Containing Compressible Mean Flow.* NASA CR-145209, 1977.

19. Abrahamson, A. L.: Acoustic Duct Liner Optimization Using Finite Elements. AIAA-79-0662, Mar. 1979.

20. Watson, W. R.; and Myers, M. K.: Inflow-Outflow Boundary Conditions for Two-Dimensional Acoustic Waves in Channels With Flow. *AIAA J.*, vol. 29, no. 9, Sept. 1991, pp. 1383–1389.

21. Snider, Royce W.: Attenuation Predictions for Segmented Liners in Supersonic Flow. M.S. Thesis, George Washington Univ., July 1993.

22. Anderson, Dale A.; Tannehill, John C.; and Pletcher, Richard H.: *Computational Fluid Mechanics and Heat Transfer.* Hemisphere Publ. Corp., 1984.

23. Myers, M. K.: On the Acoustic Boundary Condition in the Presence of Flow. *J. Sound & Vib.*, vol. 71, no. 3, Aug. 8, 1980, pp. 429–434.

24. Zienkiewicz, O. C.: *The Finite Element Method in Engineering Science.* McGraw-Hill Book Co., Inc., 1971.

25. Desai, Chandrakant S.; and Abel, John F.: *Introduction to the Finite Element Method—A Numerical Method for Engineering Analysis.* Van Nostrand Reinhold Co., 1972.

26. Horowitz, S. J.; Sigman, R. K.; and Zinn, B. T.: An Iterative Finite Element-Integral Technique for Predicting Sound Radiation From Turbofan Inlets in Steady Flight. AIAA-82-0124, Jan. 1982.

27. Baumeister, K. J.: *Utilizing Numerical Techniques in Turbofan Inlet Acoustic Suppressor Design.* NASA TM-82994, 1982.

28. Eversman, Walter: Energy Flow Criteria for Acoustic Propagation in Ducts With Flow. *J. Acoust. Soc. America,* vol. 49, no. 6, pt. 1, June 1971, pp. 1717–1721.

Appendix

Nonreflecting Condition for Inflow and Outflow Boundaries

In this appendix, elements for the coefficient matrix $[Z]$ in equations (11) of the body of this report are derived. Boundary conditions assume that the transverse component of the mean velocity v_0 is identically zero and p_0, T_0, and ρ_0 are constant. The mean flow u_0 is considered a function of the transverse coordinate only and the disturbance is assumed homentropic. Finally, the boundary is assumed to terminate in an atmosphere that is homogeneous in the axial direction. Under these assumptions, the solutions to equations (3) in the form of outgoing waves are of the following complex exponential form:

$$\tilde{\rho}(x, y) = \sum_{m=1}^{M} A_m \frac{P_m(y)}{c_0^2} e^{iK_m x} \tag{A1}$$

$$\tilde{u}(x, y) = \sum_{m=1}^{M} B_m U_m(y) e^{iK_m x} \tag{A2}$$

$$\tilde{v}(x, y) = \sum_{m=1}^{M} D_m V_m(y) e^{iK_m x} \tag{A3}$$

$$\tilde{p}(x, y) = \sum_{m=1}^{M} A_m P_m(y) e^{iK_m x} \tag{A4}$$

Here, K_m is the axial propagation constant and $U_m(y)$, $V_m(y)$, and $P_m(y)$ are the eigenfunctions associated with the axial component of acoustic velocity, transverse component of acoustic velocity, and acoustic pressure, respectively. Note that each series has been truncated at a finite number M, where M is the number of nodes along the boundary. To ensure no reflections, the sums in equations (A1)–(A4) are taken only over modes whose axial propagation constant possesses positive imaginary parts.

A nonreflecting condition relating the acoustic pressure and axial velocity at a boundary node is now developed from these series expansions. Substitution of equations (A1)–(A4) into the second component of equations (3) and elimination of $\tilde{v}$ give

$$\sum_{m=1}^{M} \left\{ i[\omega + K_m u_0(y)] B_m U_m + \frac{iK_m A_m P_m}{\rho_0} - \frac{u_0'(y) A_m P_m'(y)}{i\rho_0[\omega + K_m u_0(y)]} \right\} = 0 \tag{A5}$$

Multiplying equation (A5) by each $P_n(y)$ and integrating across the boundary give

$$\int_0^H \sum_{m=1}^{M} \left\{ i[\omega + K_m u_0(y)] B_m U_m + \frac{iK_m A_m P_m(y)}{\rho_0} - \frac{u_0'(y) A_m P_m'(y)}{i\rho_0[\omega + K_m u_0(y)]} \right\} P_n(y) \, dy = 0 \tag{A6}$$

Equation (A6) consists of M equations in $2M$ unknowns that may be expressed in matrix format as

$$\{A\} = [Z_B]\{B\} \qquad \{A\} = \left\{ \begin{array}{c} A_1 \\ A_2 \\ \vdots \\ A_M \end{array} \right\} \qquad \{B\} = \left\{ \begin{array}{c} B_1 \\ B_2 \\ \vdots \\ B_M \end{array} \right\} \tag{A7}$$

$$[Z_B] = -\begin{bmatrix} a_{11} & a_{12} & \ldots & a_{1M} \\ a_{21} & a_{22} & \ldots & a_{2M} \\ \vdots & \vdots & \ddots & \vdots \\ a_{M1} & a_{M2} & \ldots & a_{MM} \end{bmatrix}^{-1} \begin{bmatrix} b_{11} & b_{12} & \ldots & b_{1M} \\ b_{21} & b_{22} & \ldots & b_{2M} \\ \vdots & \vdots & \ddots & \vdots \\ b_{M1} & b_{M2} & \ldots & b_{MM} \end{bmatrix} \tag{A8}$$

$$a_{mn} = \int_0^H i[\omega + K_m u_0(y)] U_m(y) P_n(y)\, dy \tag{A9}$$

$$b_{mn} = \int_0^H \left\{ \frac{iK_m}{\rho_0} P_m(y) - \frac{u_0'(y)}{i\rho_0[\omega + K_m u_0(y)]} P_m'(y) \right\} P_n(y)\, dy \tag{A10}$$

The vectors $\{PB\}$ and $\{UB\}$ in equations (11) are

$$\{PB\} = [P][E]\{A\} \tag{A11}$$

$$\{UB\} = [U][E]\{B\} \tag{A12}$$

$$[E] = \begin{bmatrix} e^{iK_1 x} & 0 & \ldots & 0 \\ 0 & e^{iK_2 x} & \ldots & 0 \\ \vdots & \vdots & \ddots & \vdots \\ 0 & 0 & \ldots & e^{iK_M x} \end{bmatrix} \tag{A13}$$

$$[P] = \begin{bmatrix} P_1(y_1) & P_2(y_1) & \ldots & P_M(y_1) \\ P_1(y_2) & P_2(y_2) & \ldots & P_M(y_2) \\ \vdots & \vdots & \ddots & \vdots \\ P_1(y_M) & P_2(y_M) & \ldots & P_M(y_M) \end{bmatrix} \tag{A14}$$

$$[U] = \begin{bmatrix} U_1(y_1) & U_2(y_1) & \ldots & U_M(y_1) \\ U_1(y_2) & U_2(y_2) & \ldots & U_M(y_2) \\ \vdots & \vdots & \ddots & \vdots \\ U_1(y_M) & U_2(y_M) & \ldots & U_M(y_M) \end{bmatrix} \tag{A15}$$

in which the point $y = y_I$ corresponds to a boundary node point and x corresponds to the axial location of the boundary. Substitution of equation (A7) into equation (A11) gives

$$\{PB\} = [P][E][Z_B]\{B\} \tag{A16}$$

Solution of equation (A12) for $\{B\}$ and substitution into equation (A16) give

$$\{PB\} = [Z]\{UB\} \tag{A17}$$

$$[Z] = [P][E][Z_B][E]^{-1}[U]^{-1} \tag{A18}$$

Equations (A17) and (A18) are the nonreflecting boundary conditions referred to in the body of this report. This general condition is not dependent upon the sound source. The matrix $[Z]$

can be determined provided that each of the M eigenfunctions $P_m(y)$, $U_m(y)$, and axial wave numbers K_m is known.

The equations governing these eigenfunctions are obtained by substituting the axially propagating wave solution into equations (3) and (7) to obtain

$$i[\omega + K_m u_0(y)]U_m + \frac{iK_m P_m}{\rho_0} + u'_0(y)V_m = 0 \tag{A19}$$

$$i[\omega + K_m u_0(y)]P_m + \rho_0 c_0^2(iK_m U_m + V'_m) = 0 \tag{A20}$$

$$V_m = -\frac{P'_m}{i\rho_0[\omega + K_m u_0(y)]} \tag{A21}$$

$$V_m(0) = \frac{-1}{Z_0}\left[1 + \frac{u_0(0)K_m}{\omega}\right]P_m(0) \tag{A22}$$

$$V_m(H) = \frac{1}{Z_H}\left[1 + \frac{u_0(H)K_m}{\omega}\right]P_m(H) \tag{A23}$$

The first order system governed by equations (A19)–(A23) may be integrated numerically to obtain the eigenfunctions and axial wave number required to construct $[Z]$.

As an alternative to solving the first order system of equations (A19)–(A23), the equations may be combined into an equivalent second order system for the acoustic pressure eigenfunction

$$P''_m(y) + \left[\frac{-2K_m M'_0(y)}{k + K_m M_0(y)}\right]P'_m(y) + \{k^2 - K_m^2\left[1 - M_0^2(y)\right] + 2kK_m M_0(y)\}P_m(y) = 0 \tag{A24}$$

$$P'_m(0) = \frac{-ik\rho_0 c_0}{Z_0}\left[1 + \frac{K_m}{k}\right]^2 P_m(0) \tag{A25}$$

$$P'_m(H) = \frac{ik\rho_0 c_0}{Z_H}\left[1 + \frac{K_m}{k}\right]^2 P_m(H) \tag{A26}$$

where the mean flow Mach number $M_0(y)$ and free space wave number k is defined by the equations

$$k = \frac{\omega}{c_0} \qquad M_0(y) = \frac{u_0(y)}{c_0} \tag{A27}$$

This second order system may be integrated numerically to obtain the pressure eigenfunction $P_m(y)$ and axial decay rate K_m. Equations (A20) and (A21) are then solved to obtain the eigenfunctions $U_m(y)$ and $V_m(y)$.

The derivation of $[Z]$ is of interest for the special case of a uniform mean flow for which u_0 is a constant along the boundary. Because the mean flow gradient term u'_0 vanishes,

$$P_m(y) = \left[\frac{-\rho_0(\omega + K_m u_0)}{K_m}\right]U_m(y)$$

$$b_{mn} = -a_{mn}$$

14

Thus, $[Z_B] = [I]$ where $[I]$ is the identity matrix and $[P]$ and $[U]$ are related through a diagonal matrix $[Z_u]$

$$[P] = [U][Z_u] \tag{A28}$$

$$[Z_u] = \begin{bmatrix} -\frac{\rho_0(\omega+K_1 u_0)}{K_1} & 0 & \cdots & 0 \\ 0 & -\frac{\rho_0(\omega+K_2 u_0)}{K_2} & \cdots & 0 \\ \vdots & \vdots & \ddots & \vdots \\ 0 & 0 & \cdots & -\frac{\rho_0(\omega+K_M u_0)}{K_M} \end{bmatrix} \tag{A29}$$

For the special case of uniform flow, equation (A18) gives

$$[Z] = [P][U]^{-1} \tag{A30}$$

Elimination of $[U]$ from equation (A30) gives

$$[Z] = [P][Z_u][P]^{-1} \tag{A31}$$

Equation (A31) is the matrix $[Z]$ for no reflections in a uniform flow.
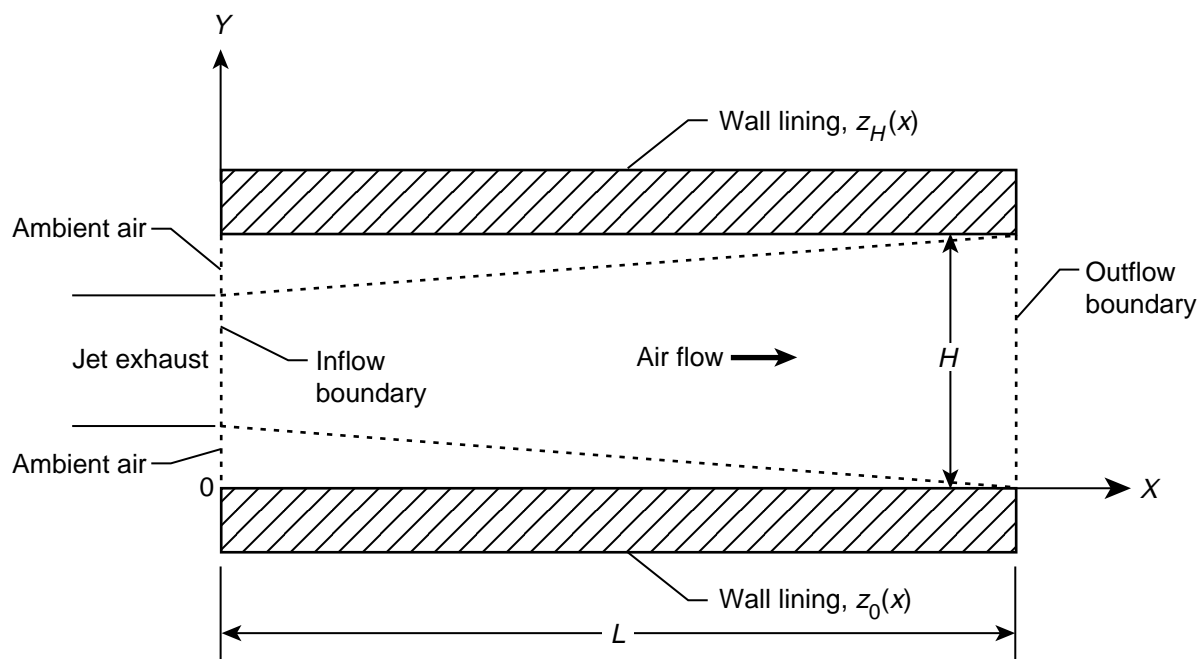
Figure 1. Exhaust jet enshrouded by lined ejector.
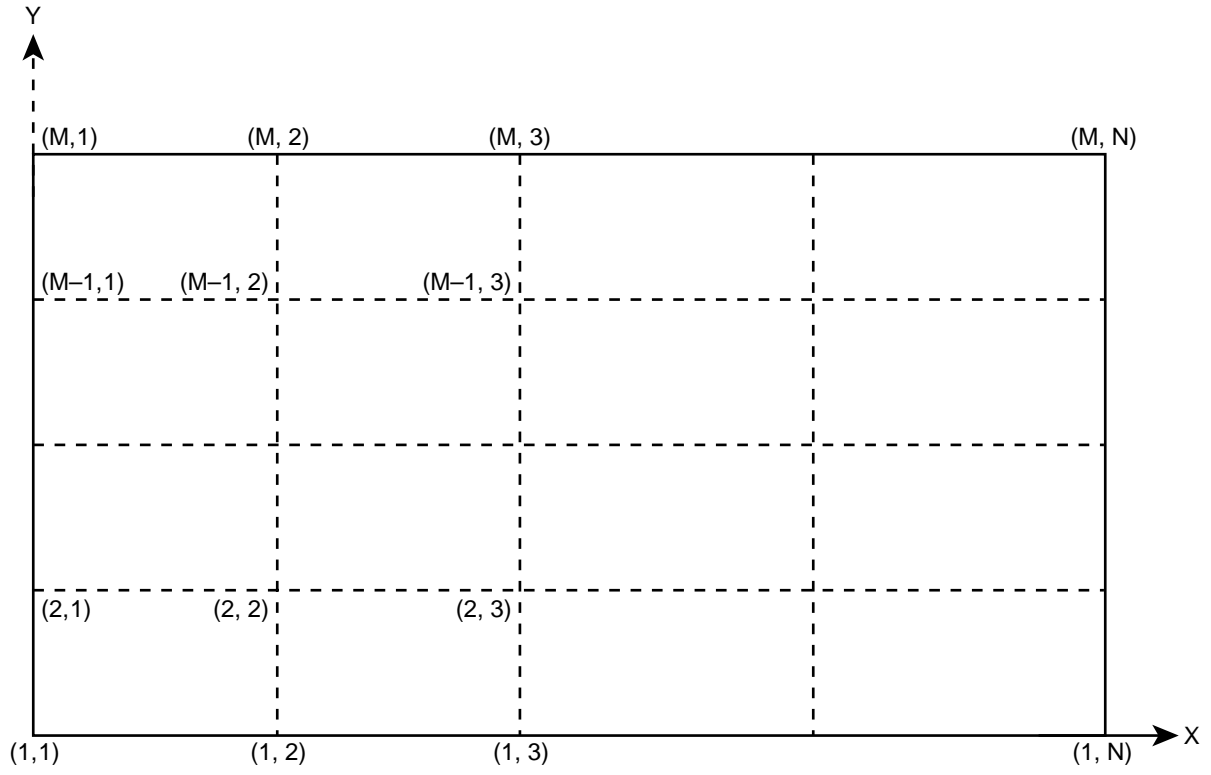
(a) Nodal numbering system.
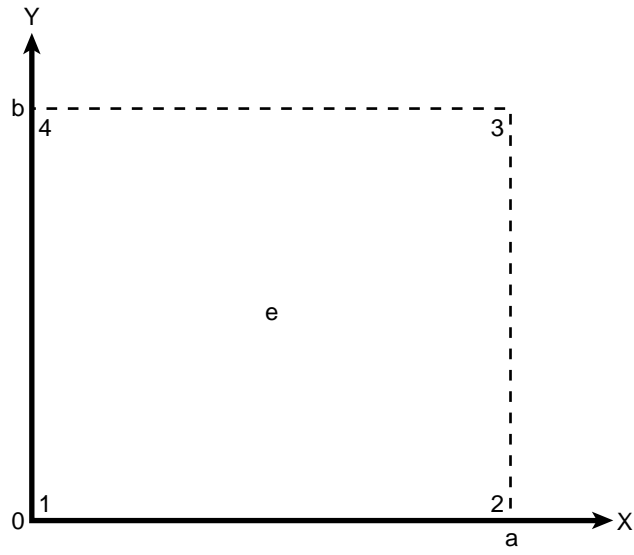
(b) Typical finite element e.

Figure 2. Finite element method acoustic field representation.
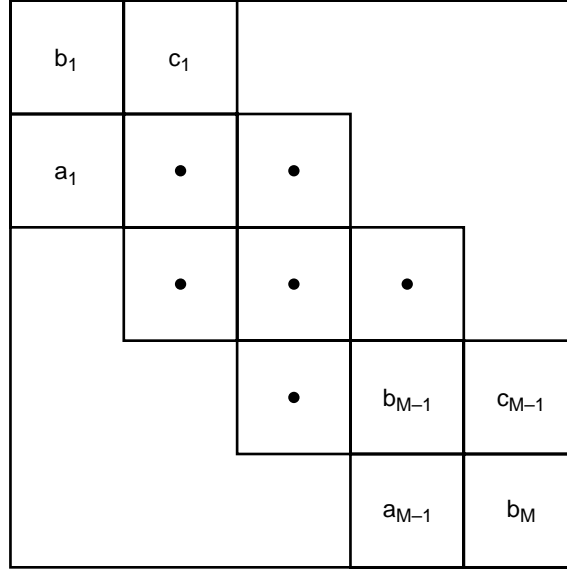
(a) Global stiffness matrix $[A]$ with major blocks.
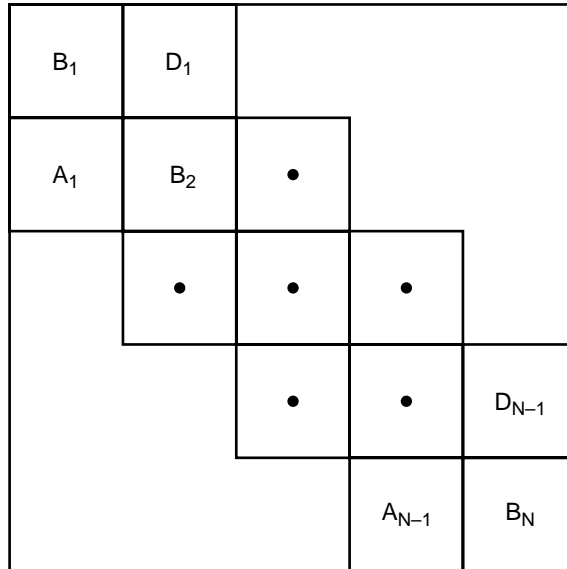
(b) Each major block in matrix $[A]$.
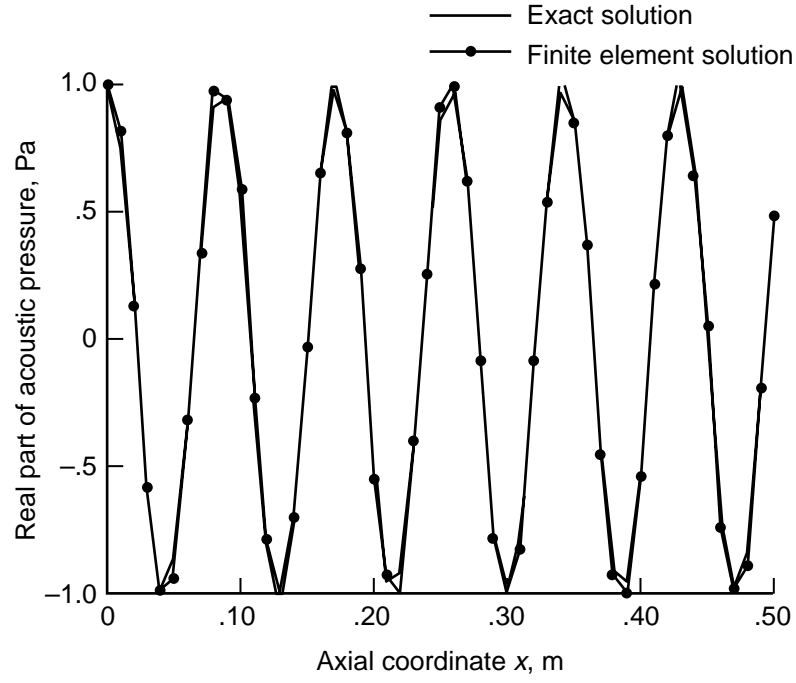
Figure 3. Block tridiagonal structure.
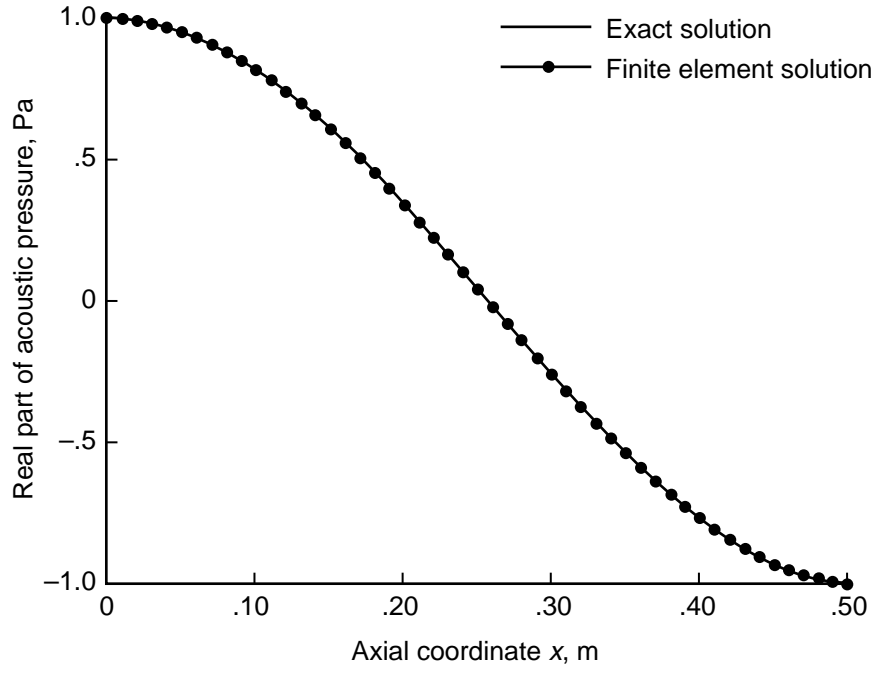
(a) Real solution.
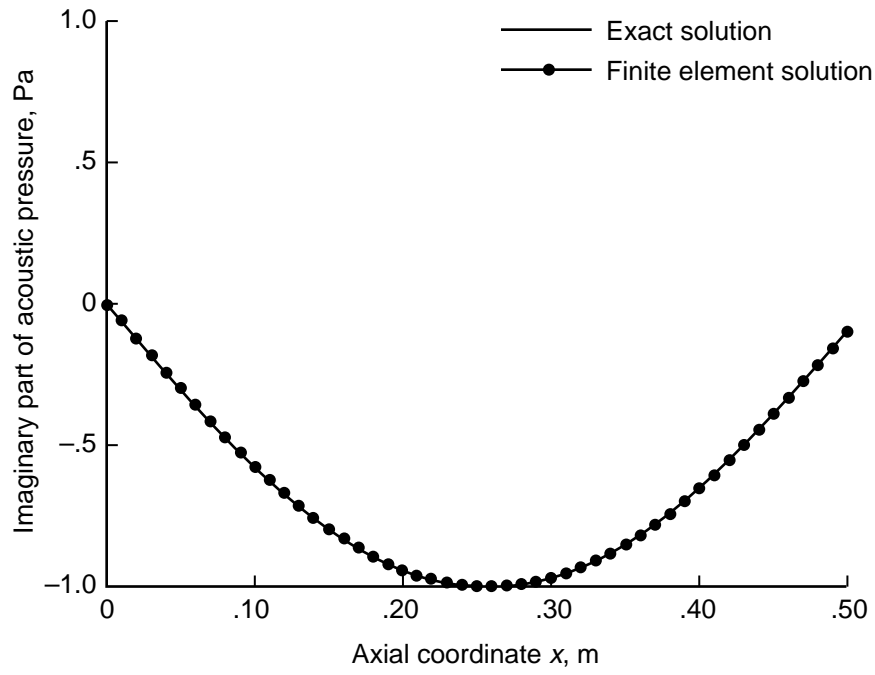
(b) Imaginary solution.

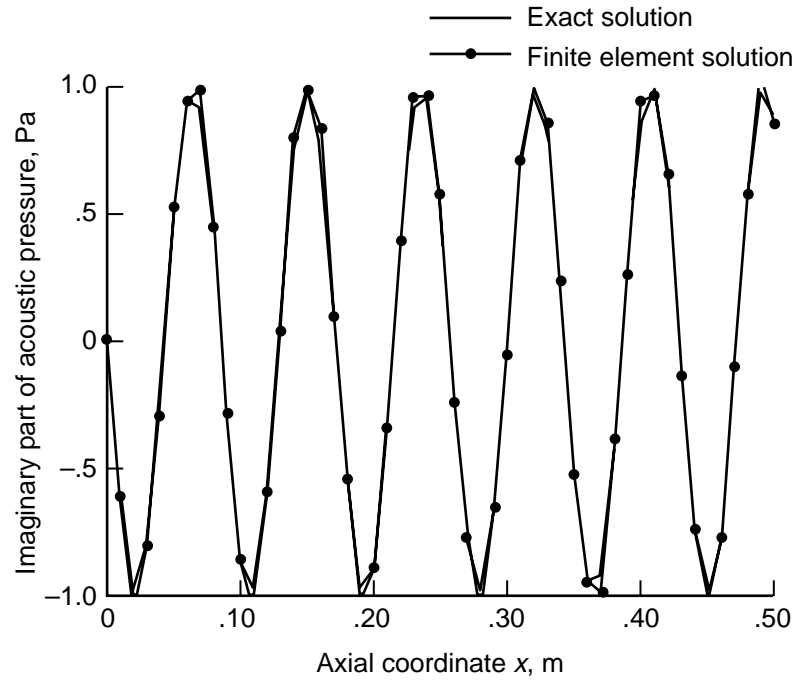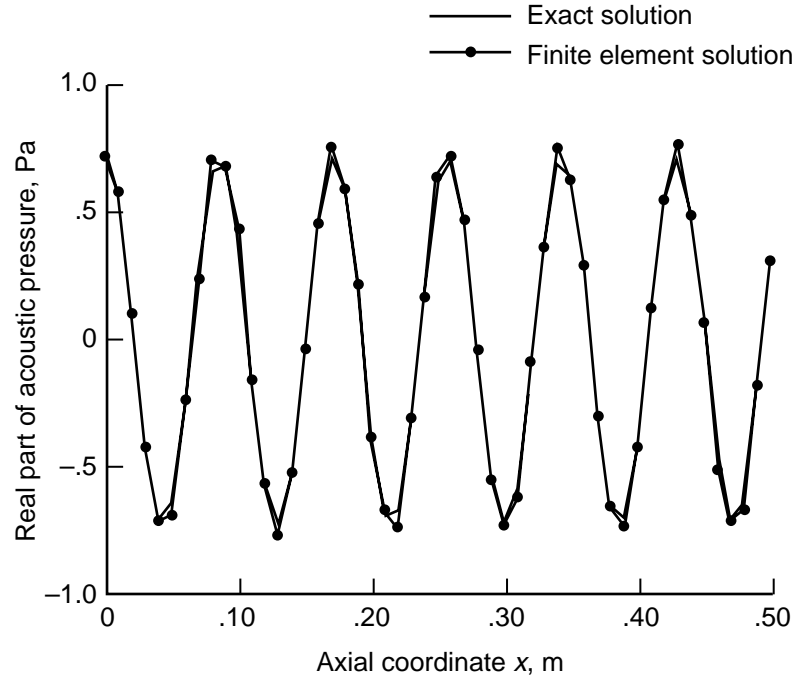Figure 4. Comparison of planar acoustic pressure at 500 Hz and $M_0 = 0.5$.
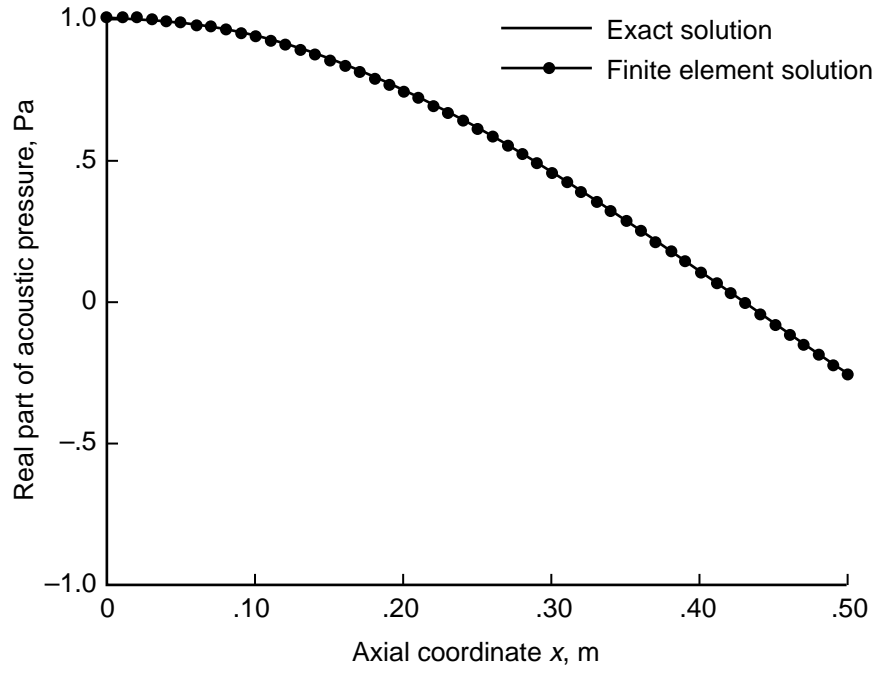
(a) Real solution.
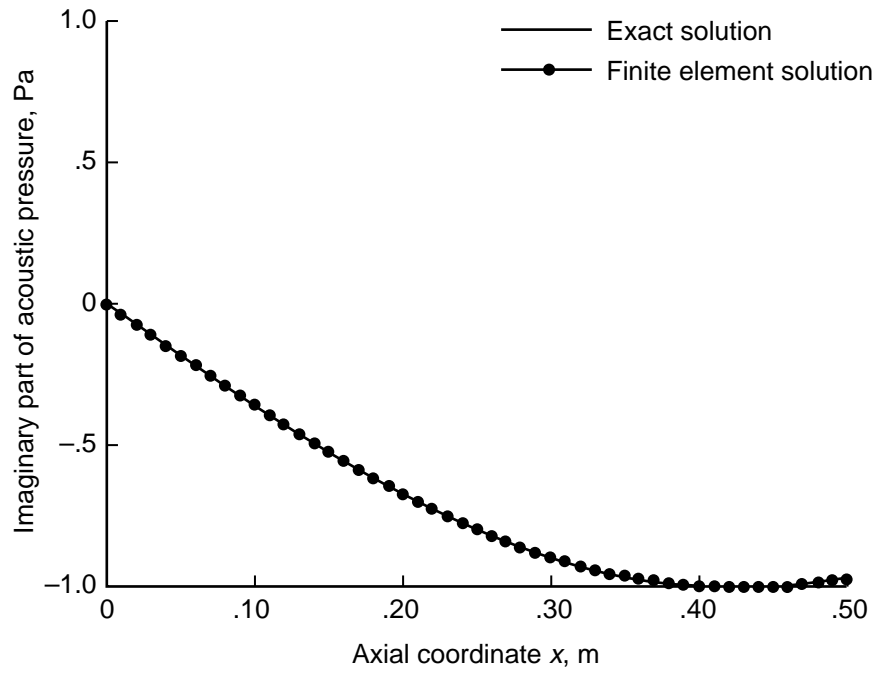
(b) Imaginary solution.

Figure 5. Comparison of planar acoustic pressure at 500 Hz and $M_0 = 1.5$.
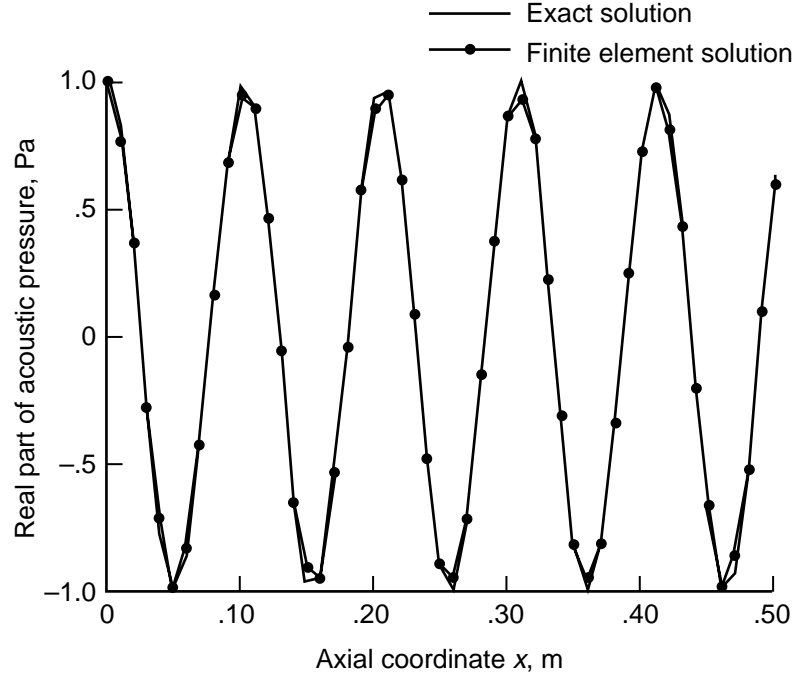
(a) Real solution.
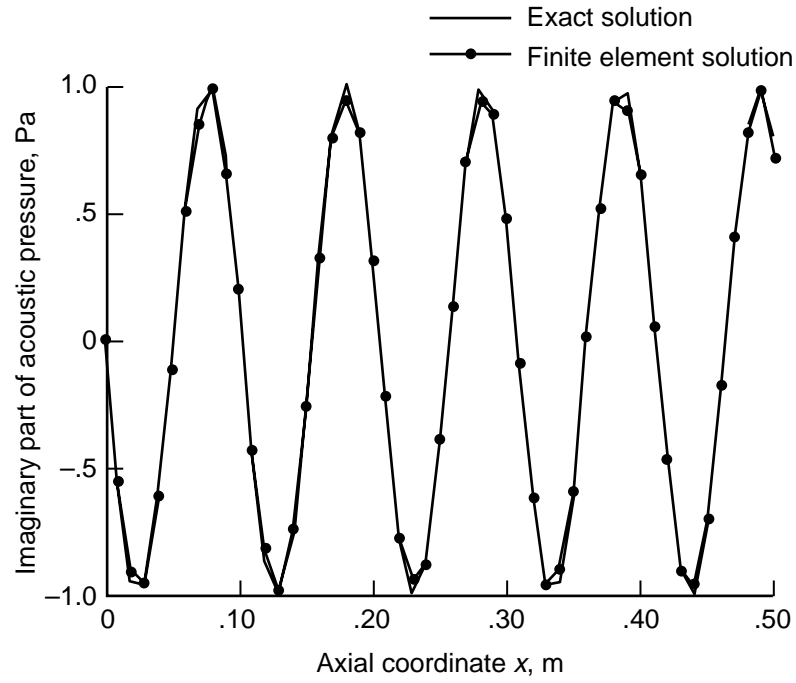
(b) Imaginary solution.

Figure 6. Comparison of planar acoustic pressure at 5000 Hz and $M_0 = 0.5$.
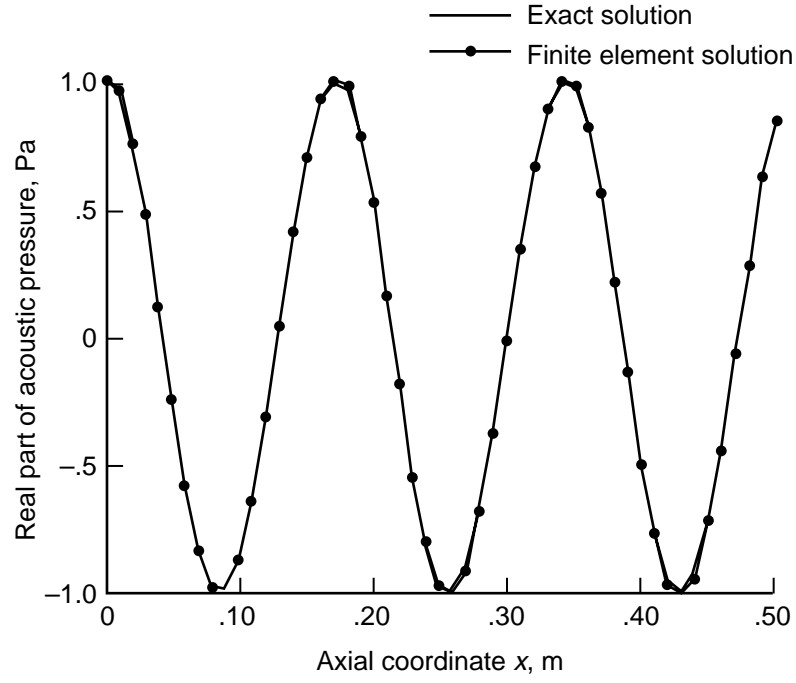
(a) Real solution.
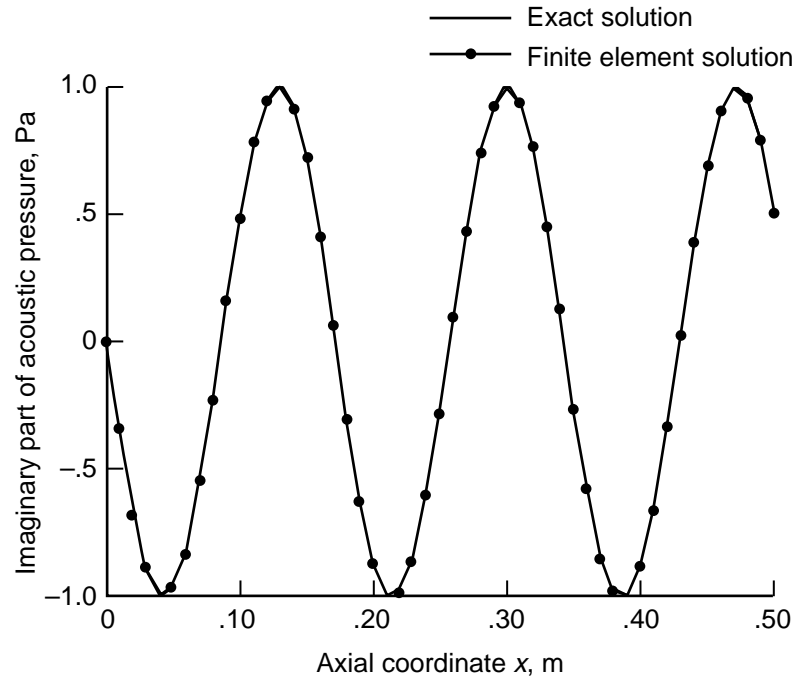
(b) Imaginary solution.

Figure 7. Comparison of planar acoustic pressure at 5000 Hz and $M_0 = 1.5$.

24

(a) Real solution.

(b) Imaginary solution.

Figure 8. Comparison of planar acoustic pressure at $10\,000$ Hz and $M_0 = 1.5$.
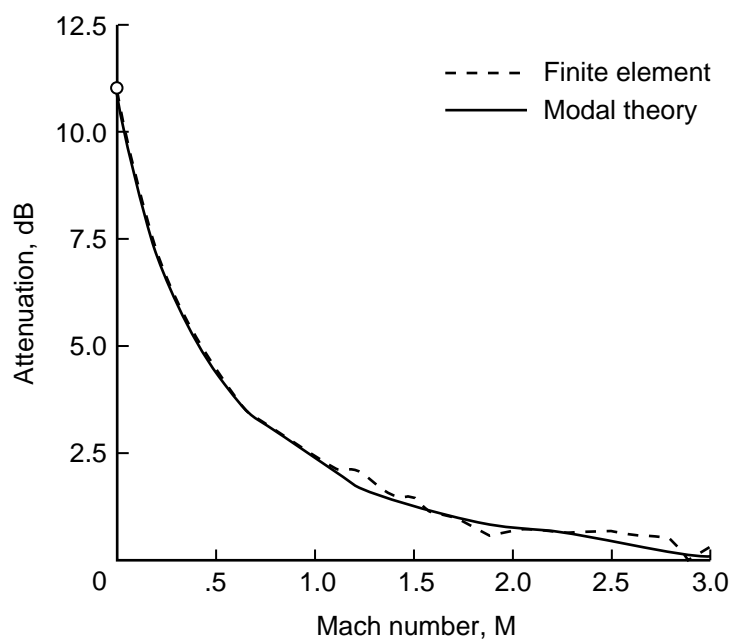
(a) Real solution.
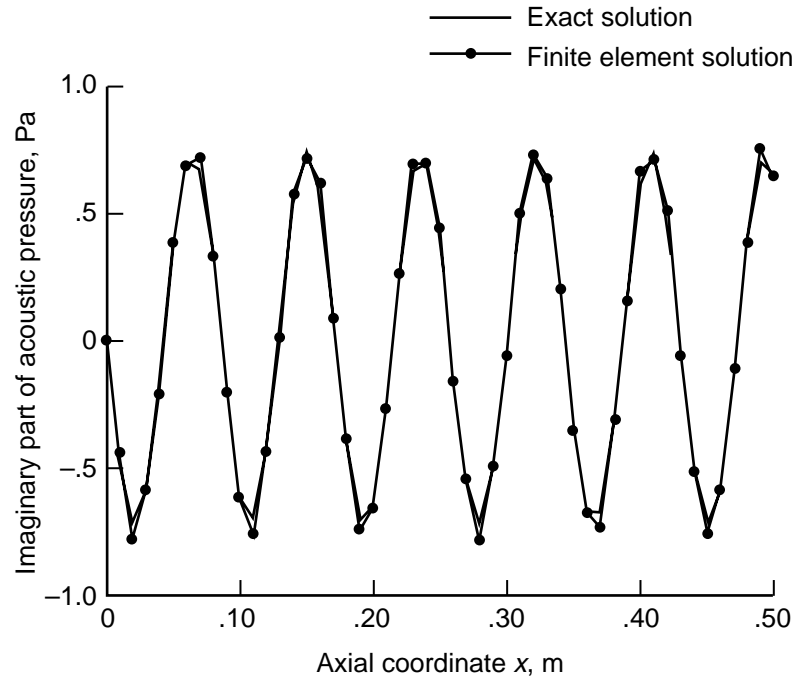
(b) Imaginary solution.

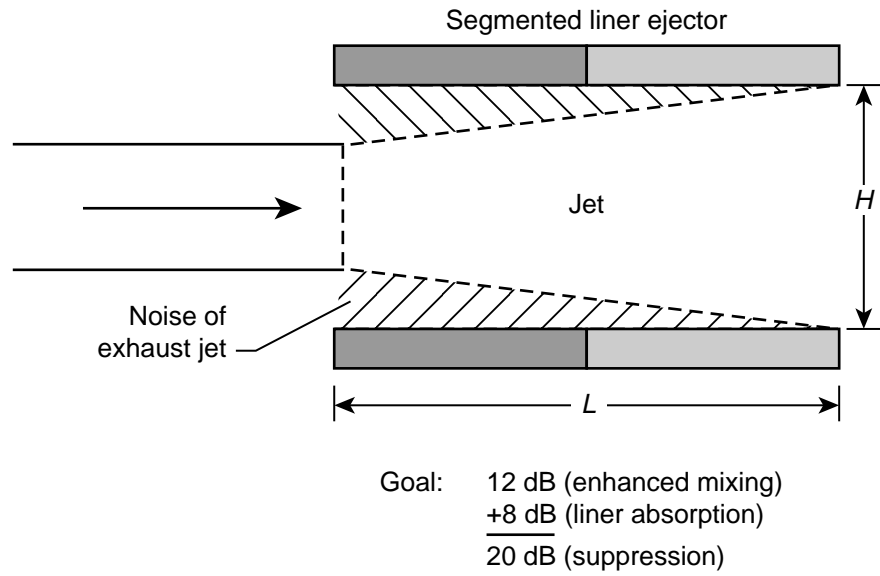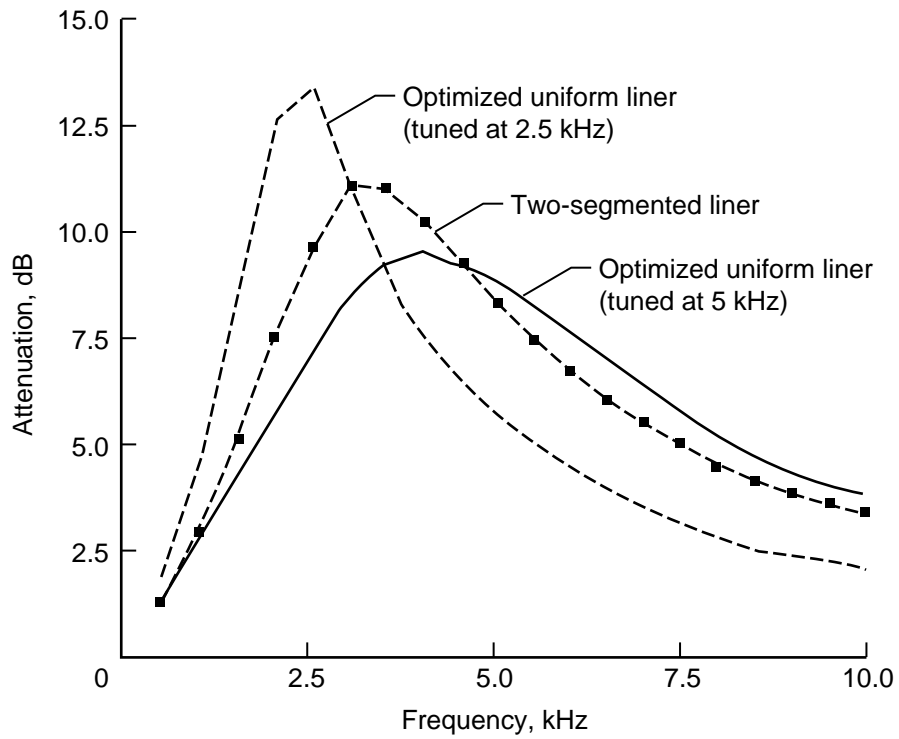Figure 9. Comparison of nonplanar acoustic pressure at 10 000 Hz and $M_0 = 1.5$.

26

Figure 10. Comparison of liner attenuation of a planar noise source at 1500 Hz with outgoing wave termination impedance.

Segmented liner ejector

Jet

Noise of
exhaust jet

H

L

Goal: 12 dB (enhanced mixing)
         +8 dB (liner absorption)
         20 dB (suppression)

(a) Variable impedance model cross section.

Optimized uniform liner
(tuned at 2.5 kHz)

Two-segmented liner

Optimized uniform liner
(tuned at 5 kHz)

Attenuation, dB

Frequency, kHz

(b) Attenuation with two-segment unoptimized liner; $M_0 = 1.5$.

Figure 11. Segmented liner for improved broadband performance.

REPORT DOCUMENTATION PAGE

1. AGENCY USE ONLY(Leave blank)	2. REPORT DATE	3. REPORT TYPE AND DATES COVERED
	April 1994	Technical Paper

4. TITLE AND SUBTITLE
A Mathematical Model for Simulating Noise Suppression of Lined Ejectors

5. FUNDING NUMBERS
WU 505-59-52-02

6. AUTHOR(S)
Willie R. Watson

7. PERFORMING ORGANIZATION NAME(S) AND ADDRESS(ES)
NASA Langley Research Center
Hampton, VA 23681-0001

8. PERFORMING ORGANIZATION REPORT NUMBER
L-17283

9. SPONSORING/MONITORING AGENCY NAME(S) AND ADDRESS(ES)
National Aeronautics and Space Administration
Washington, DC 20546-0001

10. SPONSORING/MONITORING AGENCY REPORT NUMBER
NASA TP-3425

11. SUPPLEMENTARY NOTES

12a. DISTRIBUTION/AVAILABILITY STATEMENT

Unclassified–Unlimited

Subject Category 71

12b. DISTRIBUTION CODE

13. ABSTRACT (Maximum 200 words)
A mathematical model containing the essential features embodied in the noise suppression of lined ejectors is presented. Although some simplification of the physics is necessary to render the model mathematically tractable, the current model is the most versatile and technologically advanced at the current time. A system of linearized equations and the boundary conditions governing the sound field are derived starting from the equations of fluid dynamics. A nonreflecting boundary condition is developed. In view of the complex nature of the equations, a parametric study requires the use of numerical techniques and modern computers. A finite element algorithm that solves the differential equations coupled with the boundary condition is then introduced. The numerical method results in a matrix equation with several hundred thousand degrees of freedom that is solved efficiently on a supercomputer. The model is validated by comparing results either with exact solutions or with approximate solutions from other works. In each case, excellent correlations are obtained. The usefulness of the model as an optimization tool and the importance of variable impedance liners as a mechanism for achieving broadband suppression within a lined ejector are demonstrated.

14. SUBJECT TERMS
Lined ejectors; Finite elements; Variable impedance liners; Supersonic flows; Sound attenuation; Broadband performance; Nonreflecting boundary conditions

15. NUMBER OF PAGES
29

16. PRICE CODE
A03

17. SECURITY CLASSIFICATION OF REPORT	18. SECURITY CLASSIFICATION OF THIS PAGE	19. SECURITY CLASSIFICATION OF ABSTRACT	20. LIMITATION OF ABSTRACT
Unclassified	Unclassified		